

Imidazo[1,2-*a*]pyrimidine as a New Antileishmanial Pharmacophore against *Leishmania amazonensis* Promastigotes and Amastigotes

Ravinder Kumar, Rahul Singh, Ayla das Chagas Almeida, Juliana da Trindade Granato, Ari Sérgio de Oliveira Lemos, Kushvinder Kumar, Madhuri T. Patil, Adilson D. da Silva, Ambadas B. Rode, Elaine S. Coimbra,* and Deepak B. Salunke*



Cite This: *ACS Omega* 2023, 8, 40613–40621



Read Online

ACCESS |



Metrics & More

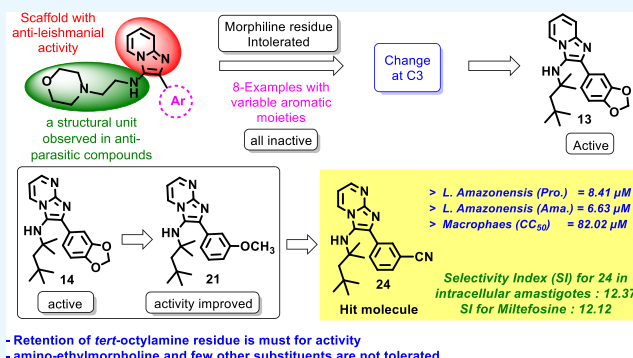


Article Recommendations



Supporting Information

ABSTRACT: *Leishmania* poses a substantial threat to the human population all over the globe because of its visceral and cutaneous spread engendered by all 20 species. Unfortunately, the available drugs against leishmania are already hobbled with toxicity, prolonged treatment, and increasing instances of acquisition of resistance. Under these grave circumstances, the development of new drugs has become imperative to keep these harmful microbes at bay. To this end, a Groebke–Blackburn–Bienaymé multi-component reaction-based library of different imidazo-fused heterocycles has been synthesized and screened against *Leishmania amazonensis* promastigotes and amastigotes. Among the library compounds, the imidazo-pyrimidine **24** has been found to be the most effective (inhibitory concentration of 50% (IC_{50}) < 10 μ M), with selective antileishmanial activity on amastigote forms, a stage of the parasite related to human disease. The compound **24** has exhibited an IC_{50} value of 6.63 μ M, being \sim two times more active than miltefosine, a reference drug. Furthermore, this compound is >10 times more destructive to the intracellular parasites than host cells. The observed in vitro antileishmanial activity along with suitable in silico physicochemical and absorption, distribution, metabolism, excretion, and toxicity (ADMET) properties of compound **24** reinforce the imidazo-pyrimidine scaffold as a new antileishmanial pharmacophore and encourage further murine experimental leishmaniasis studies.



1. INTRODUCTION

Leishmaniasis is an endemic disease in 98 countries worldwide, transmitted to humans and other mammals by the bite of female phlebotomine sandflies, affecting mainly the Americas, East and North Africa, and West and Southeast Asia.¹ The protozoan of the genus *Leishmania* is the etiological agent of leishmaniasis, a complex of clinical manifestations ranging from nonfatal cutaneous ulcerations to the disfiguring mucocutaneous form and the potential fatal visceral leishmaniasis.² The pathology of this disease depends on several factors, such as the *Leishmania* species and the host's immunobiological response.³

The therapies available for the treatment of leishmaniasis are very limited. Pentavalent antimonials, amphotericin B, pentamidine, and paromomycin, are currently available drugs. However, these medications are quite toxic and require long-term parenteral administration. Additionally, low therapeutic effectiveness in some endemic areas has been reported due to the emergence of resistant strains.^{4,5} Miltefosine, originally developed for the treatment of metastatic cutaneous breast carcinoma, is the only drug approved for the oral treatment of leishmaniasis. However, this medication is teratogenic and

shows variability in efficacy.⁴ Therefore, the search for new drugs that are less toxic to the patient and more effective against leishmaniasis is required.

Nitrogen heterocycles are the key molecules to be explored in the field of leishmaniasis. Major classes of these heterocyclic moieties involve the quinoline, triazole, pyrazole, imidazole, indole, pyrimidine, β -carboline, quinoxaline, quinazoline, and benzimidazole. Among the various fused imidazole-based scaffolds, imidazo-pyrimidine has shown promising results against trypanosomatida species, including *Leishmania*.^{6–9} In particular, 6,8-dibromo-3-nitro-2-phenyl sulfonyl methyl imidazo[1,2-*a*]pyrimidine (**1**, Figure 1) has shown better antileishmanial activity than the marketed drug miltefosine and pentamidine against *Leishmania donovani* promastigotes.⁶ Antileishmanial screening of 2,3-diarylimidazo[1,2-*a*]pyrimidine series of compounds has

Received: July 26, 2023

Accepted: September 26, 2023

Published: October 20, 2023



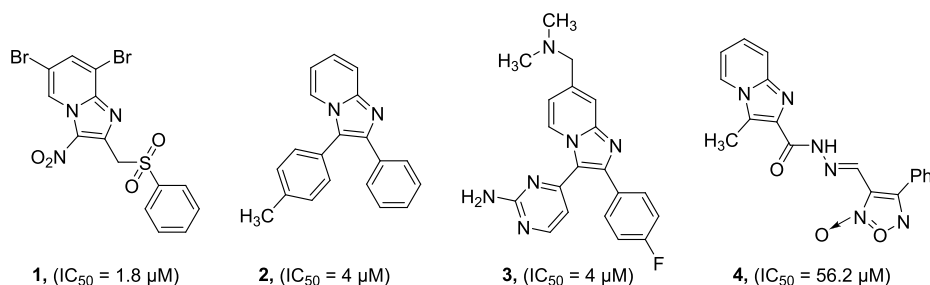


Figure 1. Imidazo-pyridine-based molecules having antileishmanial activity.

Scheme 1. General Synthetic Protocol for the Formation of Imidazo-Fused Heterocycles.

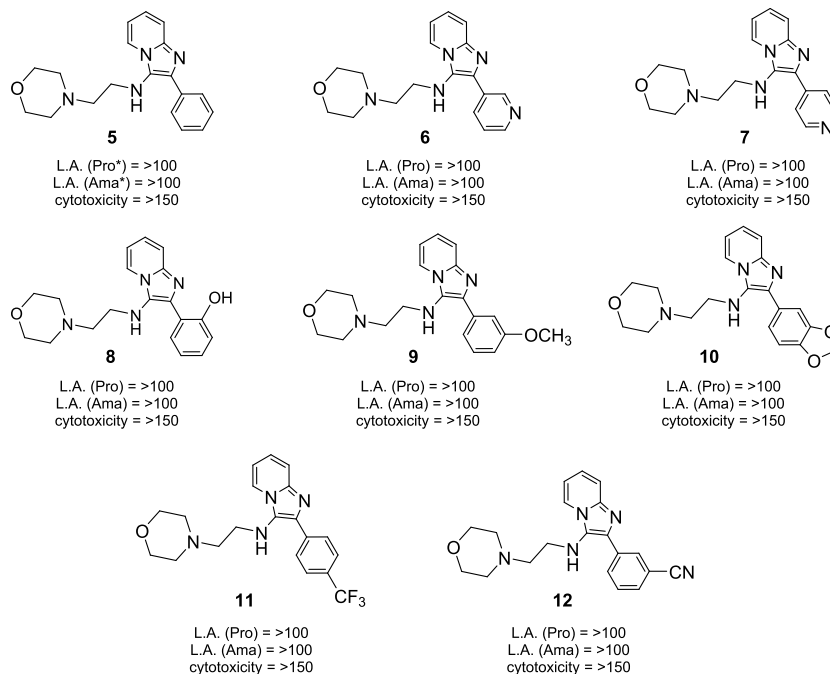
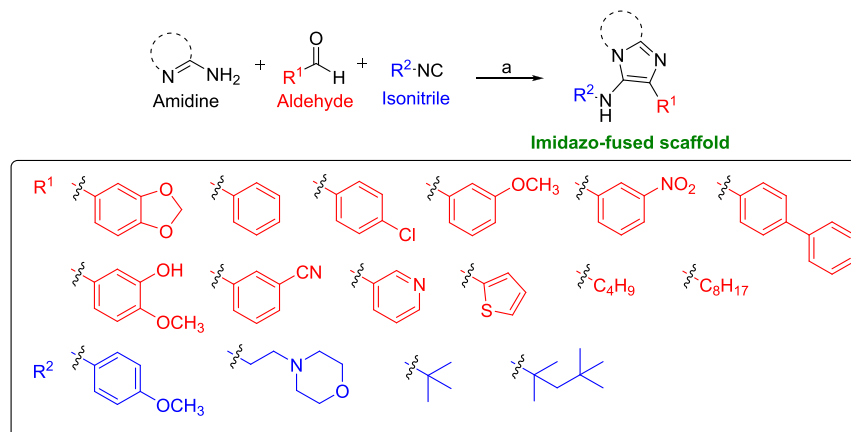


Figure 2. Antileishmanial activity and cytotoxicity of imidazo-pyridine analogues (in μM). Pro and ama mean promastigotes and amastigotes, respectively, of *L. amazonensis* (L.A.). Cytotoxicity is the toxic effect on murine macrophages. These results correspond to the average of three experiments performed in duplicate.

resulted in a 2-phenyl-3-(*p*-tolyl)imidazo[1,2-*a*]pyridine (2) as the most potent analogue against amastigote stages of *Leishmania major* with inhibitory concentration (IC_{50}) = 4 μM .⁷ A C2-, C3-, and C7-trisubstituted imidazo-pyridine (3) has also demonstrated promising antileishmanial activity against *L. major* ($IC_{50} = 0.2 \mu M$),⁸ whereas another imidazo-

pyridine-based compound (4) is found to be active against *Trypanosoma cruzi* amastigotes ($IC_{50} = 56.2 \mu M$).⁹

The literature survey reveals the promising utility of a fused imidazo-pyridine scaffold¹⁰ for the discovery of new anti-leishmanial agents, and the active analogues demonstrate a diverse substitution tolerability at C2 and C3 positions as well

as on the pyridine ring for the improved activity. Groebke–Blackburn–Bienaymé (GBB) multicomponent reaction (MCR) provides an easy access to construct a diverse set of imidazo-fused heterocycles in a single step utilizing different amidines, isonitriles, and aldehydes.^{11–19} In order to identify new antileishmanial agents, a new GBB-MCR-based library has been evaluated against *Leishmania amazonensis* promastigotes and amastigotes, and physicochemical and absorption, distribution, metabolism, excretion, and toxicity (ADMET) properties have been examined with a view to predict important information about imidazo-pyridine analogues.

2. RESULTS AND DISCUSSION

A small library of imidazo-pyridines (compounds 5–12, Figure 2) was synthesized via GBB-MCR (Scheme 1) using 2-aminopyridine, aldehydes, and 4-(2-isocyanoethyl)morpholine.²⁰

2.1. Reagent and Conditions. HCl in dioxane (4M), CH₃CN, and MW (110 °C), 20 min. Morpholine is an important privileged structure due to its wide range of medicinal and pharmacological participations. Antiparasitic²¹ and specifically antileishmanial activities^{22–25} of morpholine-bearing compounds has motivated us to use 4-(2-isocyanoethyl)morpholine as a tool to attach 4-(2-aminoethyl)morpholine residue at the C3 position of our designed scaffold. The synthesized compound library has been screened against *L. amazonensis* promastigotes and amastigotes, and the toxicity has also been evaluated on macrophages (Figure 2).

Although the synthesized compounds (5–12, Figure 2) have shown no toxic effect on macrophages (cytotoxic concentration capable of inhibiting 50% (CC₅₀) > 150 μM), unfortunately, none of them have shown any antileishmanial activity at the maximum concentration tested (100 μM). Considering the importance of pyrimidine along with the application of benzodioxole in medicinal chemistry, two more analogues (13 and 14, Figure 3) have been synthesized using 1,1,3,3-tetramethylbutyl isocyanide, benzodioxole aldehyde, and 2-aminopyrimidine or 2-aminopyridine components.

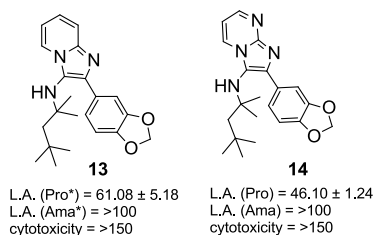


Figure 3. Antileishmanial activity and cytotoxicity of compounds 13 and 14 (in μM). Pro and ama mean promastigotes and amastigotes, respectively, of *L. amazonensis* (L.A.). Cytotoxicity is the toxic effect on murine macrophages. These results correspond to the average of three experiments performed in duplicate.

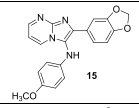
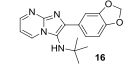
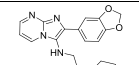
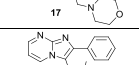
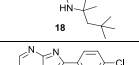
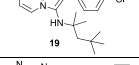
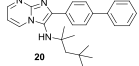
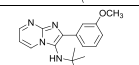
Interestingly, compound 14 has shown a positive result against *L. amazonensis* promastigotes (IC₅₀ = 46.10 μM) suggesting the importance of the 3-(1,1,3,3-tetramethylbutylamine) residue at the C3 position of the imidazo[1,2-*a*]pyrimidine scaffold. It is noteworthy to observe that none of these active compounds showed any cytotoxicity to the macrophages. In the *Leishmania* species, the variation in sensitivity between promastigote and amastigote forms has

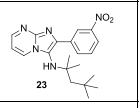
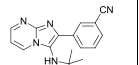
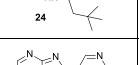
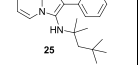
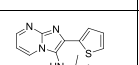
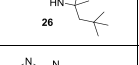
been previously reported not only for new drugs but also for well-known antileishmanial drugs, such as amphotericin B, paromomycin, pentavalent antimonials, and miltefosine.²⁶ The different drug susceptibility profiles are unclear, and they may be associated with many factors: (i) unlike promastigotes, amastigotes are intracellular parasites and found inside the macrophage parasitophorous vacuole, whose pH is acidic, and this can interfere in uptake/inactivation of the compound by host cell, (ii) different metabolic pathways of biological stages, and (iii) proteomic differences involved in important processes, among others.^{25–28}

Based on these results and in order to obtain new compounds with promising antileishmanial activity, a series of new derivatives were synthesized with focus on compound 14, an imidazo-pyrimidine analogue (Table 1). First, changes were made at the C3 position of imidazo-pyrimidine by retaining the 1,3-benzodioxole residue. The activity was lost in each case (15–17, Table 1). Then, by preserving the 3-(1,1,3,3-tetramethylbutylamine) substitution at the C3 position of imidazo-pyrimidine, changes were made at the C2 position. Phenyl substitution (18, Table 1) in place of furfuryl at position 2 retained the activity against *L. amazonensis* promastigotes while showed more potency against the intramacrophage biological stages. The 4-chloro phenyl (19, Table 1) and biphenyl (20, Table 1) substituents enhanced the activity against both forms of the parasite. The compound with the 3-methoxy phenyl group (21, Table 1) showed an increase in the activity against both parasite forms, while the 3-hydroxy and 4-methoxy phenyl group (22, Table 1) was not tolerated for the antileishmanial activity. The C3-nitro phenyl-substituted analogue (23, Table 1) did not show any biological activity, but the 3-cyano phenyl analogue (24, Table 1) was found to be the most potent antileishmanial molecule in the series, with IC₅₀ values <10 μM. Besides the capacity to inhibit the growth of promastigotes (IC₅₀ = 8.41 μM), the compound 24 also exhibited good activity against intracellular amastigotes (IC₅₀ = 6.63 μM), being more effective than miltefosine (IC₅₀ = 15.05 and 12.52 μM, respectively), used as the reference drug. In addition, the lead compound 24 was 10 times more toxic to the parasite than to the host cell (CC₅₀ = 82.02 μM and selectivity index (SI) = 12.37), with a profile similar to that of miltefosine (CC₅₀ = 151.81 μM and SI = 12.12). It was interesting to note that in compound 24 along with a few more analogues (18, 22, and 25) when assayed on MCF-7, MDA-MB-231, and HEP-G2 cell lines at 25 μM, no any significant cytotoxicity was observed (Supporting Information Figure S65).²⁹ Although these cell lines were mostly used for anticancer assays, they were cell lines of human origin, and therefore, these data also reinforced the negligible toxicity by compound 24 to mammalian cells. Further, the replacement of the 3-cyanophenyl group by the 3-pyridinyl group (25, Table 1) evaded the activity, but the 2-thiophenyl group (26, Table 1) showed an effect on *L. amazonensis* amastigotes only. 2-Butyl- and 2-octyl-substituted products (27 and 28, Table 1) demonstrated moderate activity against *L. amazonensis* promastigotes and amastigotes.

In vitro results have stimulated future studies for assessing the activity of compounds in the in vivo model. However, it is important to predict the druggability of the new compound using computational tools. On the grounds that compound 24 has shown higher in vitro antileishmanial activity and a selective action (SI > 10), its physicochemical and ADMET

Table 1. Activity of Imidazo-Pyrimidine Analogues in *L. amazonensis* Promastigote and Amastigote Forms and Cytotoxicity on Murine Peritoneal Macrophages

Entry	Compound	Cytotoxicity on macrophages CC ₅₀ (μM) ^a	Promastigotes IC ₅₀ (μM) ^b	Intracellular amastigotes IC ₅₀ (μM) ^b	Selectivity Index ^c
1		>150	>100	>100	ND
2		>150	>100	>100	ND
3		>150	>100	>100	ND
4		76.72 ± 4.2	50.27 ± 4.9	25.70 ± 0.68	2.98
5		>150	36.44 ± 0.92	34.91 ± 0.79	>4.29
6		39.66 ± 1.96	31.09 ± 0.46	16.94 ± 1.5	2.34
7		57.12 ± 2.88	17.02 ± 1.05	18.39 ± 0.90	3.10
8		>150	>100	>100	ND

Entry	Compound	Cytotoxicity on macrophages CC ₅₀ (μM) ^a	Promastigotes IC ₅₀ (μM) ^b	Intracellular amastigotes IC ₅₀ (μM) ^b	Selectivity Index ^c
9		>150	>100	>100	ND
10		82.02 ± 5.5	8.41 ± 0.83	6.63 ± 0.41	12.37
11		>150	>100	>100	ND
12		>150	>100	45.55 ± 5.6	>3.29
13		32.70 ± 1.49	47.77 ± 2.6	28.14 ± 0.98	1.16
14		54.01 ± 2.7	40.61 ± 0.87	32.08 ± 1.3	1.68
15	Miltefosine	151.81 ± 0.03	15.05 ± 2.08	12.52 ± 0.83	12.12

^aValues of CC₅₀. ^bValues of IC₅₀. ^cSI: CC₅₀ in peritoneal macrophages/IC₅₀ in intracellular amastigotes. ND means not determined. Miltefosine was used as the reference drug. These results correspond to the average of three experiments performed in duplicate.

properties are evaluated. The results obtained through the PKCSM software point out compound **24** with excellent oral bioavailability (Table 2), since it does not violate any of the

Table 2. In Silico Physicochemical Properties of 24

compound	molecular weight	logP	hydrogen acceptors	hydrogen donors	violations
24	347.466	4.89468	5	1	0

parameters of the Lipinski's rule of five ($\log P \leq 5$; $M_W \leq 500$, hydrogen bond acceptor (HBA) ≤ 5 , and hydrogen bond donor (HBD) ≤ 10).³⁰ These parameters are associated with a good solubility and intestinal permeability that comprise the first step of drug absorption.³¹

For successful medications, ADMET profiles are critical, and the in silico pharmacokinetic prediction is a good tool in the early development process of the drug discovery.³² The ADMET profile of compound **24** by AdmetSAR has predicted a good intestinal absorption (Table 3), corroborating with the physicochemical analysis. In addition, favorable results are obtained for the topical administration of compound **24** (Table 3). This route reduces systemic adverse effects and can also be utilized to obtain regulated or delayed drug delivery.³³ Also, the in silico prediction has revealed that the lead compound **24** is a substrate/inhibitor of several CYP450 enzymes, which are key enzymes in the liver.³⁴ The CYP450 superfamily is the most prevalent phase-I drug-metabolizing enzyme, responsible for converting drugs into water-soluble compounds, facilitating their excretion by the kidney and/or liver.³⁴ Thus, these data suggest that compound **24** is likely to

Table 3. ADMET Profile of 24

absorption	intestinal absorption	yes
absorption	skin permeability	yes
distribution	BBB permeability	yes
distribution	CNS permeability	yes
metabolism	CYP2D6 substrate	no
metabolism	CYP3A4 substrate	yes
metabolism	CYP1A2 inhibitor	yes
metabolism	CYP2C19 inhibitor	yes
metabolism	CYP2C9 inhibitor	yes
metabolism	CYP2D6 inhibitor	yes
metabolism	CYP3A4 inhibitor	no
excretion	renal OCT2 substrate	yes
toxicity	AMES toxicity	yes
Toxicity	Hepatotoxicity	Yes
Toxicity	Skin Sensitization	No

undergo hepatic metabolism to be excreted later. The kidney, in turn, is a very important organ participating in the process of eliminating substances with organic cation transporters (OCTs) and multidrug and toxin extrusion proteins (MATEs), which are considered as the major transporters that secrete cationic drugs into the urine.³⁵ Therefore, our results suggest that after hepatic metabolism, compound **24** can be excreted by OCTs in the kidney. Toxicology parameter is the last aspect in the ADMET profile examined, and the analysis has suggested that compound **24** exhibits liver and mutagenic toxicities. Thus, we consider that, if the oral route is chosen for in vivo model, these data should be better investigated in the preclinical trial phases. On the other

hand, since no skin toxicity has been observed, a possible topical application can be explored.

CONCLUSIONS

In summary, twenty four imidazo-fused derivatives were synthesized and evaluated against *L. amazonensis* species. Among the compounds tested, compound **24** exhibited expressive activity against promastigote and amastigote forms of *L. amazonensis* and did not show significant toxic effects on mammalian cells. In addition, physicochemical and ADMET studies indicated that compound **24** could be used through oral or topical administration. These data stimulated further studies of the efficacy of this compound in murine experimental leishmaniasis.

4. EXPERIMENTAL SECTION

4.1. Chemistry. **4.1.1. General.** Commercially available reagents were used without any further purification. 2-Aminopyridine, 2-aminopyrimidine, and 2-aminothiazole were purchased from Sigma, while 2-aminopyrazine was purchased from Avra Synthesis. Further, aldehydes—benzaldehyde, butanal, 3-cyanobenzaldehyde, 2-hydroxybenzaldehyde, 3-hydroxy-4-methoxybenzaldehyde, 3-methoxybenzaldehyde, and thiopene-2-carbaldehyde—were also purchased from Avra Synthesis. In addition, aldehydes such as pyridine-3-carbaldehyde, pyridine-4-carbaldehyde, piperonal, 4-phenylbenzaldehyde, 3-nitrobenzaldehyde, and octanal were procured from Sigma, while 4-chlorobenzaldehyde and 4-(trifluoromethyl)benzaldehyde were procured from CDH and TCI, respectively. Furthermore, isonitriles—*tert*-butyl isonitrile, 1,1,3,3-tetramethylbutyl isonitrile, 4-(2-isocyanoethyl)morpholine isonitrile, and 4-methoxyphenyl isonitrile—were procured from Sigma. The catalyst HCL in dioxane was obtained from Sigma. The bulk solvents such as hexanes, ethyl acetate, dichloromethane, and MeOH were distilled before use. TLC was performed on Merck silica gel F₂₅₄ aluminum sheets and viewed under UV light at 254 or 360 nm. Compounds were purified by column chromatography using a 230–400 mesh silica gel, and a MeOH–dichloromethane system was used as the mobile phase. ¹H and ¹³C NMR spectra were recorded on Bruker Avance-II 400 or 500 MHz NMR spectrometers in CDCl₃. Chemical shifts were reported in parts per million (ppm) relative to tetramethylsilane (TMS) as the internal standard. The abbreviations used in reporting spectra were as follows: s (singlet), d (doublet), t (triplet), m (multiple), dt (doublet of triplet), td (triplet of doublet), ddd (doublet of doublet of doublet), and br (broad). HPLC (Agilent 1260 Infinity-II LC system, Serial number DEABG06552; Column: Agilent 5 HC-C18(2) 150 × 4.6 mm) was used to confirm the purity (>98%) of the synthesized compounds. MS was reported on an Agilent 1290 LC/MSD single quad system or on Waters Alliance 2795, Q-TOF Micromass spectrometer. The Synthos 3000 MW reactor by Anton Paar was used for the GBB-MCRs.

4.1.2. Synthesis and Characterization of Compounds. **General Procedure for the GBB Reaction.** Amidine (200 mg, 1 equiv) was dissolved in acetonitrile (3 mL) in a microwave vessel, and aldehyde (1.5 equiv) was added to the reaction mixture followed by isonitrile (1.1 equiv). Catalytic amounts of HCL in dioxane (4M) were added to the reaction mixture. The reaction was allowed to occur in a microwave at 110 °C for 20 min in power-controlled mode (900 W). The crude

compounds were concentrated on a rotary evaporator and subjected to column chromatography purification. The compounds were eluted with MeOH/DCM (0–5%) using a 230–400 mesh silica gel.

N-(2-morpholinoethyl)-2-(pyridin-3-yl)imidazo[1,2-*a*]-pyridin-3-amine (**6**). ¹H NMR (500 MHz, CDCl₃) δ 9.27 (dd, *J* = 2.2, 0.7 Hz, 1H), 8.54 (dd, *J* = 4.8, 1.6 Hz, 1H), 8.41–8.29 (m, 1H), 8.12 (dt, *J* = 6.9, 1.0 Hz, 1H), 7.55 (d, *J* = 9.1 Hz, 1H), 7.37 (ddd, *J* = 7.9, 4.8, 0.7 Hz, 1H), 7.16 (ddd, *J* = 9.0, 6.7, 1.2 Hz, 1H), 6.82 (td, *J* = 6.8, 1.0 Hz, 1H), 3.97 (s, 1H), 3.80–3.62 (m, 4H), 3.22–2.99 (m, 2H), 2.61–2.50 (m, 2H), 2.50–2.33 (m, 4H). ¹³C NMR (126 MHz, CDCl₃) δ 148.1, 148.0, 141.9, 134.3, 132.2, 130.5, 127.0, 124.3, 123.6, 122.4, 117.6, 112.0, 66.9, 58.30, 53.7, 44.2. MS-ESI [(M+H)⁺]: *m/z* calculated for C₁₈H₂₂N₅O⁺: 324.2; found: 324.2.

N-(2-morpholinoethyl)-2-(pyridin-4-yl)imidazo[1,2-*a*]-pyridin-3-amine (**7**). ¹H NMR (500 MHz, CDCl₃) δ 8.63 (dd, *J* = 4.6, 1.6 Hz, 2H), 8.11 (dt, *J* = 6.9, 1.1 Hz, 1H), 7.98 (dd, *J* = 4.6, 1.6 Hz, 2H), 7.56 (dt, *J* = 9.0, 0.9 Hz, 1H), 7.17 (ddd, *J* = 9.1, 6.6, 1.3 Hz, 1H), 6.82 (td, *J* = 6.8, 1.0 Hz, 1H), 4.00 (s, 1H), 3.82–3.66 (m, 4H), 3.16–3.08 (m, 2H), 2.59–2.55 (m, 2H), 2.53–2.42 (m, 4H). ¹³C NMR (126 MHz, CDCl₃) δ 150.0, 142.0, 141.8, 131.8, 128.4, 124.7, 122.4, 120.9, 117.9, 112.2, 67.0, 58.3, 53.7, 44.1. MS-ESI [(M+H)⁺]: *m/z* calculated for C₁₈H₂₂N₅O⁺: 324.2; found: 324.2.

2-(3-((2-morpholinoethyl)amino)imidazo[1,2-*a*]pyridin-2-yl)phenol (**8**). ¹H NMR (500 MHz, CDCl₃) δ 13.01 (s, 1H), 8.10 (dt, *J* = 6.9, 1.1 Hz, 1H), 7.92 (dd, *J* = 7.8, 1.6 Hz, 1H), 7.47–7.38 (m, 1H), 7.17–7.04 (m, 2H), 6.96 (dd, *J* = 8.2, 1.2 Hz, 1H), 6.87–6.70 (m, 2H), 3.81 (s, 1H), 3.75–3.56 (m, 4H), 3.03 (s, 2H), 2.64–2.50 (m, 2H), 2.45 (s, 4H). ¹³C NMR (126 MHz, CDCl₃) δ: 158.0, 139.2, 134.2, 129.0, 125.7, 125.1, 124.5, 122.1, 118.7, 117.7, 117.3, 116.7, 112.3, 67.0, 58.5, 53.8, 43.8. MS-ESI [(M+H)⁺]: *m/z* calculated for C₁₉H₂₃N₄O₂⁺: 339.1816; found: 339.1961.

2-(3-methoxyphenyl)-*N*-(2-morpholinoethyl)imidazo[1,2-*a*]pyridin-3-amine (**9**). ¹H NMR (500 MHz, CDCl₃) δ 8.01 (d, *J* = 6.8 Hz, 1H), 7.57–7.39 (m, 3H), 7.25 (t, *J* = 7.9 Hz, 1H), 7.03 (ddd, *J* = 9.0, 6.7, 1.2 Hz, 1H), 6.84–6.74 (m, 1H), 6.69 (td, *J* = 6.8, 0.9 Hz, 1H), 3.99 (s, 1H), 3.79 (s, 3H), 3.66–3.56 (m, 4H), 3.04–2.89 (m, 2H), 2.44 (dd, *J* = 6.2, 4.8 Hz, 2H), 2.34 (s, 4H). ¹³C NMR (126 MHz, CDCl₃) δ: 159.9, 141.2, 135.6, 134.6, 129.5, 126.7, 123.9, 122.4, 119.3, 117.4, 113.0, 112.7, 111.7, 66.9, 58.3, 55.3, 53.7, 44.0. MS-ESI [(M+H)⁺]: *m/z* calculated for C₂₀H₂₅N₄O₂⁺: 353.1972; found: 353.2070.

2-(benzo[*d*][1,3]dioxol-5-yl)-*N*-(2-morpholinoethyl)imidazo[1,2-*a*]pyridin-3-amine (**10**). ¹H NMR (500 MHz, CDCl₃) δ 8.09 (d, *J* = 6.8 Hz, 1H), 7.73–7.37 (m, 3H), 7.13 (ddd, *J* = 9.0, 6.7, 1.2 Hz, 1H), 6.89 (d, *J* = 8.1 Hz, 1H), 6.79 (td, *J* = 6.8, 1.0 Hz, 1H), 5.99 (s, 2H), 3.94 (s, 1H), 3.83–3.48 (m, 4H), 3.20–2.92 (m, 2H), 2.56 (dd, *J* = 6.3, 4.8 Hz, 2H), 2.47 (s, 4H). ¹³C NMR (126 MHz, CDCl₃) δ 148.0, 147.0, 141.1, 134.7, 128.4, 125.7, 123.8, 122.3, 120.8, 117.3, 111.7, 108.5, 107.5, 101.1, 67.0, 58.3, 53.7, 43.9, 29.7. MS-ESI [(M+H)⁺]: *m/z* calculated for C₂₀H₂₃N₄O₃⁺: 367.1765; found: 367.1915.

N-(2-morpholinoethyl)-2-(4-(trifluoromethyl)phenyl)imidazo[1,2-*a*]pyridin-3-amine (**11**). ¹H NMR (500 MHz, CDCl₃) δ 8.17 (d, *J* = 8.1 Hz, 2H), 8.10 (d, *J* = 6.9 Hz, 1H), 7.67 (d, *J* = 8.2 Hz, 2H), 7.55 (d, *J* = 9.1 Hz, 1H), 7.15 (ddd, *J* = 9.0, 6.6, 1.2 Hz, 1H), 6.80 (td, *J* = 6.8, 1.0 Hz, 1H), 3.95 (s, 1H), 3.84–3.60 (m, 4H), 3.08 (s, 2H), 2.68–2.50 (m, 2H),

2.49–2.26 (m, 4H). ^{13}C NMR (126 MHz, CDCl_3) δ 141.6, 138.1, 133.4, 131.0, 129.3, 129.0, 128.8, 128.5, 127.5, 127.3, 126.9, 125.5, 125.4, 125.4, 124.3, 123.2, 122.4, 117.8, 111.9, 67.0, 58.3, 53.7, 44.1. MS-ESI $[(\text{M}+\text{H})^+]$: m/z calculated for $\text{C}_{20}\text{H}_{22}\text{F}_3\text{N}_4\text{O}^+$: 391.2; found: 391.2.

3-(3-((2-morpholinoethyl)amino)imidazo[1,2-*a*]pyridin-2-yl)benzotrile (12). ^1H NMR (500 MHz, CDCl_3) δ 8.41 (t, J = 1.4 Hz, 1H), 8.33 (dt, J = 7.7, 1.5 Hz, 1H), 8.12 (dt, J = 6.9, 1.0 Hz, 1H), 7.63–7.45 (m, 3H), 7.17 (ddd, J = 9.0, 6.7, 1.2 Hz, 1H), 6.82 (td, J = 6.8, 1.0 Hz, 1H), 3.87 (s, 1H), 3.79–3.63 (m, 4H), 3.11 (s, 2H), 2.67–2.53 (m, 2H), 2.53–2.35 (m, 4H). ^{13}C NMR (126 MHz, CDCl_3) δ 141.7, 135.9, 132.8, 130.9, 130.4, 130.3, 129.3, 127.0, 124.5, 122.4, 119.0, 117.8, 112.7, 112.1, 67.0, 58.4, 53.7, 44.1. MS-ESI $[(\text{M}+\text{H})^+]$: m/z calculated for $\text{C}_{20}\text{H}_{22}\text{N}_5\text{O}^+$: 348.2; found: 348.2.

2-(benzo[*d*][1,3]dioxol-5-yl)-*N*-(2,4,4-trimethylpentan-2-yl)imidazo[1,2-*a*]pyrimidin-3-amine (14). ^1H NMR (500 MHz, CDCl_3) δ 8.50 (dd, J = 6.8, 2.0 Hz, 1H), 8.46 (dd, J = 4.1, 2.0 Hz, 1H), 7.47 (d, J = 1.6 Hz, 1H), 7.39 (dd, J = 8.0, 1.7 Hz, 1H), 6.88 (dd, J = 7.9, 3.4 Hz, 1H), 6.82 (dd, J = 6.8, 4.1 Hz, 1H), 6.00 (s, 2H), 3.21 (s, 1H), 1.58 (s, 2H), 1.04 (s, 9H), 0.98 (s, 6H). ^{13}C NMR (126 MHz, CDCl_3) δ : 149.1, 147.7, 147.3, 144.9, 141.3, 131.0, 128.8, 122.4, 121.2, 109.2, 108.2, 107.7, 101.1, 60.9, 57.0, 31.8, 31.7, 29.0. ESI $[(\text{M}+\text{H})^+]$: m/z calculated for $\text{C}_{21}\text{H}_{27}\text{N}_4\text{O}_2^+$: 367.2129; found: 367.2319.

2-(benzo[*d*][1,3]dioxol-5-yl)-*N*-(4-methoxyphenyl)imidazo[1,2-*a*]pyrimidin-3-amine (15). ^1H NMR (500 MHz, CDCl_3) δ 8.50 (dd, J = 4.1, 2.0 Hz, 1H), 8.08 (dd, J = 6.7, 2.1 Hz, 1H), 7.62–7.58 (m, 2H), 6.81–6.75 (m, 4H), 6.53 (d, J = 9.0 Hz, 2H), 5.95 (s, 2H), 5.55 (s, 1H), 3.74 (s, 3H). ^{13}C NMR (126 MHz, CDCl_3) δ : 154.0, 150.1, 148.0, 147.9, 145.5, 140.7, 137.8, 130.4, 127.1, 121.7, 116.7, 115.6, 114.7, 108.7, 108.5, 107.9, 101.2, 55.8. MS-ESI $[(\text{M}+\text{H})^+]$: m/z calculated for $\text{C}_{20}\text{H}_{17}\text{N}_4\text{O}_3^+$: 361.1295; found: 361.1496.

2-(benzo[*d*][1,3]dioxol-5-yl)-*N*-(*tert*-butyl)imidazo[1,2-*a*]pyrimidin-3-amine (16). ^1H NMR (500 MHz, CDCl_3) δ 8.49 (dd, J = 6.8, 2.1 Hz, 1H), 8.45 (dd, J = 4.0, 2.0 Hz, 1H), 7.54 (d, J = 1.6 Hz, 1H), 7.49 (dd, J = 8.1, 1.7 Hz, 1H), 6.86 (d, J = 8.1 Hz, 1H), 6.80 (dd, J = 6.8, 4.1 Hz, 1H), 6.00 (s, 2H), 3.14 (s, 1H), 1.06 (s, 9H). ^{13}C NMR (126 MHz, CDCl_3) δ : 149.2, 147.6, 147.3, 144.9, 140.9, 130.9, 128.6, 122.3, 121.3, 108.9, 108.2, 107.7, 101.1, 56.6, 30.4. MS-ESI $[(\text{M}+\text{H})^+]$: calculated for $\text{C}_{17}\text{H}_{19}\text{N}_4\text{O}_2^+$: 311.1; found: 311.1.

2-(benzo[*d*][1,3]dioxol-5-yl)-*N*-(2-morpholinoethyl)imidazo[1,2-*a*]pyrimidin-3-amine (17). ^1H NMR (500 MHz, CDCl_3) δ 8.95 (d, J = 1.4 Hz, 1H), 7.99 (dd, J = 4.6, 1.5 Hz, 1H), 7.83 (d, J = 4.6 Hz, 1H), 7.61–7.41 (m, 2H), 6.91 (d, J = 8.5 Hz, 1H), 6.02 (s, 2H), 4.12 (s, 1H), 3.83–3.59 (m, 4H), 3.10 (s, 2H), 2.64–2.51 (m, 2H), 2.47 (s, 4H). ^{13}C NMR (126 MHz, CDCl_3) δ : 148.2, 147.6, 143.2, 137.2, 136.4, 128.9, 127.6, 127.3, 121.2, 115.1, 108.7, 107.6, 101.3, 66.9, 58.2, 53.7, 43.6, 29.7. MS-ESI $[(\text{M}+\text{H})^+]$: m/z calculated for $\text{C}_{19}\text{H}_{22}\text{N}_5\text{O}_3^+$: 368.1717; found: 368.1483.

2-phenyl-*N*-(2,4,4-trimethylpentan-2-yl)imidazo[1,2-*a*]pyrimidin-3-amine (18). ^1H NMR (500 MHz, CDCl_3) δ 8.54 (dd, J = 6.8, 2.0 Hz, 1H), 8.48 (dd, J = 4.0, 2.0 Hz, 1H), 7.96–7.83 (m, 2H), 7.44 (t, J = 7.6 Hz, 2H), 7.34 (t, J = 7.4 Hz, 1H), 6.83 (dd, J = 6.8, 4.1 Hz, 1H), 3.36 (s, 1H), 1.56 (s, 2H), 1.02 (s, 9H), 0.95 (s, 6H). ^{13}C NMR (126 MHz, CDCl_3) δ : 149.3, 145.1, 141.5, 134.7, 131.2, 128.6, 128.3, 127.9, 121.8, 107.8, 60.9, 56.9, 31.8, 31.7, 29.0. MS-ESI $[(\text{M}+\text{H})^+]$: m/z calculated for $\text{C}_{20}\text{H}_{27}\text{N}_4^+$: 323.2230; found: 323.2.

2-(4-chlorophenyl)-*N*-(2,4,4-trimethylpentan-2-yl)imidazo[1,2-*a*]pyrimidin-3-amine (19). ^1H NMR (400 MHz, CDCl_3) δ 8.27 (dd, J = 6.6, 1.9 Hz, 1H), 8.23 (dd, J = 4.3, 1.9 Hz, 1H), 7.53–7.46 (m, 2H), 7.43–7.36 (m, 2H), 6.71 (dd, J = 6.6, 4.4 Hz, 1H), 4.23 (s, 1H), 1.89 (s, 2H), 1.56 (s, 6H), 0.98 (s, 9H). ^{13}C NMR (126 MHz, CDCl_3) δ : 149.6, 145.1, 140.3, 133.7, 133.2, 131.2, 129.8, 128.5, 121.8, 107.9, 61.0, 57.0, 31.8, 31.7, 29.1. MS-ESI $[(\text{M}+\text{H})^+]$: m/z calculated for $\text{C}_{20}\text{H}_{26}\text{ClN}_4^+$: 357.1; found: 357.1.

2-([1,1'-biphenyl]-4-yl)-*N*-(2,4,4-trimethylpentan-2-yl)imidazo[1,2-*a*]pyrimidin-3-amine (20). ^1H NMR (500 MHz, CDCl_3) δ 8.54 (dd, J = 6.8, 2.0 Hz, 1H), 8.49 (dd, J = 4.0, 2.0 Hz, 1H), 8.02 (d, J = 8.4 Hz, 2H), 7.81–7.57 (m, 4H), 7.46 (t, J = 7.7 Hz, 2H), 7.35 (t, J = 7.4 Hz, 1H), 6.83 (dd, J = 6.8, 4.1 Hz, 1H), 3.32 (s, 1H), 1.60 (s, 2H), 1.04 (s, 9H), 0.99 (s, 6H). ^{13}C NMR (126 MHz, CDCl_3) δ : 149.3, 145.2, 141.1, 140.7, 140.5, 133.7, 131.1, 129.0, 128.8, 127.4, 127.0, 126.9, 121.9, 107.8, 61.0, 57.0, 31.9, 31.7, 29.1. MS-ESI $[(\text{M}+\text{H})^+]$: m/z calculated for $\text{C}_{26}\text{H}_{31}\text{N}_4^+$: 399.2; found: 399.3.

2-(3-methoxyphenyl)-*N*-(2,4,4-trimethylpentan-2-yl)imidazo[1,2-*a*]pyrimidin-3-amine (21). ^1H NMR (400 MHz, CDCl_3) δ 8.53 (dd, J = 6.8, 2.1 Hz, 1H), 8.49 (dd, J = 4.1, 2.1 Hz, 1H), 7.53 (dd, J = 2.5, 1.5 Hz, 1H), 7.46–7.40 (m, 1H), 7.34 (t, J = 7.9 Hz, 1H), 6.90 (ddd, J = 8.2, 2.6, 1.0 Hz, 1H), 6.84 (dd, J = 6.8, 4.1 Hz, 1H), 3.88 (s, 3H), 3.29 (s, 1H), 1.58 (s, 2H), 1.03 (s, 9H), 0.96 (s, 6H). ^{13}C NMR (126 MHz, CDCl_3) δ : 159.7, 149.3, 145.0, 141.3, 136.1, 131.2, 129.1, 121.9, 121.0, 114.2, 113.7, 107.8, 60.9, 56.9, 55.4, 31.8, 31.7, 29.0. MS-ESI $[(\text{M}+\text{H})^+]$: m/z calculated for $\text{C}_{21}\text{H}_{29}\text{N}_4\text{O}^+$: 353.2; found: 353.2.

2-methoxy-5-(3-((2,4,4-trimethylpentan-2-yl)amino)imidazo[1,2-*a*]pyrimidin-2-yl)phenol (22). ^1H NMR (500 MHz, CDCl_3) δ 8.51 (dd, J = 6.8, 2.0 Hz, 1H), 8.47 (dd, J = 4.0, 2.0 Hz, 1H), 7.53 (d, J = 2.0 Hz, 1H), 7.42 (dd, J = 8.3, 2.0 Hz, 1H), 6.91 (d, J = 8.4 Hz, 1H), 6.83 (dd, J = 6.8, 4.1 Hz, 1H), 3.92 (s, 3H), 3.29 (s, 1H), 1.57 (s, 2H), 1.03 (s, 9H), 0.96 (s, 6H). ^{13}C NMR (126 MHz, CDCl_3) δ : 149.0, 146.7, 145.5, 144.9, 141.3, 131.1, 127.9, 121.4, 120.7, 115.1, 110.7, 107.7, 60.9, 56.9, 55.9, 31.8, 31.7, 29.0. MS-ESI $[(\text{M}+\text{H})^+]$: m/z calculated for $\text{C}_{21}\text{H}_{29}\text{N}_4\text{O}_2^+$: 369.2; found: 369.2.

2-(3-nitrophenyl)-*N*-(2,4,4-trimethylpentan-2-yl)imidazo[1,2-*a*]pyrimidin-3-amine (23). ^1H NMR (400 MHz, CDCl_3) δ 9.02–8.93 (m, 1H), 8.59–8.50 (m, 2H), 8.50–8.42 (m, 1H), 8.18 (ddd, J = 8.2, 2.3, 1.0 Hz, 1H), 7.62 (t, J = 8.0 Hz, 1H), 6.90 (dd, J = 6.7, 4.1 Hz, 1H), 3.19 (s, 1H), 1.65 (s, 2H), 1.05 (s, 9H), 1.02 (s, 6H). MS-ESI $[(\text{M}+\text{H})^+]$: m/z calculated for $\text{C}_{20}\text{H}_{26}\text{N}_5\text{O}_2^+$: 368.2; found: 368.2.

3-(3-((2,4,4-trimethylpentan-2-yl)amino)imidazo[1,2-*a*]pyrimidin-2-yl)benzotrile (24). ^1H NMR (500 MHz, CDCl_3) δ 8.59–8.47 (m, 2H), 8.36 (s, 1H), 8.28 (d, J = 7.8 Hz, 1H), 7.61 (d, J = 7.7 Hz, 1H), 7.55 (t, J = 7.8 Hz, 1H), 6.89 (dd, J = 6.5, 4.3 Hz, 1H), 3.22 (s, 1H), 1.60 (s, 2H), 1.04 (s, 9H), 0.99 (s, 6H). ^{13}C NMR (126 MHz, CDCl_3) δ : 150.2, 145.3, 139.1, 136.1, 132.7, 132.0, 131.3, 131.2, 129.2, 122.2, 118.8, 112.3, 108.3, 61.0, 57.1, 31.8, 31.7, 29.2. MS-ESI $[(\text{M}+\text{H})^+]$: m/z calculated for $\text{C}_{21}\text{H}_{26}\text{N}_5^+$: 348.2; found: 348.2.

2-(pyridin-3-yl)-*N*-(2,4,4-trimethylpentan-2-yl)imidazo[1,2-*a*]pyrimidin-3-amine (25). ^1H NMR (400 MHz, CDCl_3) δ 9.19 (d, J = 1.3 Hz, 1H), 8.58 (dd, J = 4.7, 1.3 Hz, 1H), 8.56–8.47 (m, 2H), 8.35 (dt, J = 7.9, 1.7 Hz, 1H), 7.41 (dd, J = 7.8, 4.8 Hz, 1H), 6.88 (dd, J = 6.6, 4.2 Hz, 1H), 3.28 (s, 1H), 1.59 (s, 2H), 1.03 (s, 9H), 0.99 (s, 6H). ^{13}C NMR (126 MHz, CDCl_3) δ : 149.9, 149.2, 148.7, 145.5, 138.5, 135.9, 131.3,

130.9, 123.5, 122.3, 108.1, 60.9, 57.0, 31.8, 31.7, 29.1. MS-ESI [(M+H)⁺]: *m/z* calculated for C₁₉H₂₆N₅⁺: 324.2; found: 324.2.

2-(thiophen-2-yl)-N-(2,4,4-trimethylpentan-2-yl)imidazo[1,2-a]pyrimidin-3-amine (26). ¹H NMR (400 MHz, CDCl₃) δ 8.54–8.33 (m, 2H), 7.64 (dd, *J* = 3.6, 1.1 Hz, 1H), 7.35 (dd, *J* = 5.1, 1.1 Hz, 1H), 7.11 (dd, *J* = 5.1, 3.6 Hz, 1H), 6.81 (dd, *J* = 6.8, 4.1 Hz, 1H), 3.25 (s, 1H), 1.69 (s, 2H), 1.12 (s, 6H), 1.08 (s, 9H). MS-ESI [(M+H)⁺]: *m/z* calculated for C₁₈H₂₅N₄S⁺: 329.1; found: 329.1.

2-butyl-N-(2,4,4-trimethylpentan-2-yl)imidazo[1,2-a]pyrimidin-3-amine (27). ¹H NMR (400 MHz, CDCl₃) δ 8.54–8.28 (m, 2H), 6.77 (dd, *J* = 6.7, 4.1 Hz, 1H), 3.32 (s, 1H), 2.82–2.69 (m, 2H), 1.79 (tt, *J* = 7.8, 6.8 Hz, 2H), 1.65 (s, 2H), 1.47–1.31 (m, 2H), 1.15 (s, 6H), 1.08 (s, 9H), 0.93 (t, *J* = 7.4 Hz, 3H). ESI [(M+H)⁺]: *m/z* calculated for C₁₈H₃₁N₄⁺: 303.2; found: 303.2.

2-octyl-N-(2,4,4-trimethylpentan-2-yl)imidazo[1,2-a]pyrimidin-3-amine (28). ¹H NMR (400 MHz, CDCl₃) δ 8.50–8.31 (m, 2H), 6.79 (dd, *J* = 6.5, 4.3 Hz, 1H), 3.95 (s, 1H), 2.81–2.70 (m, 2H), 1.85–1.75 (m, 2H), 1.66 (s, 2H), 1.35–1.23 (m, 10H), 1.15 (s, 6H), 1.09 (s, 9H), 0.86 (t, *J* = 6.9 Hz, 3H). ¹³C NMR (126 MHz, CDCl₃) δ 148.4, 145.1, 143.8, 130.7, 121.5, 107.4, 59.8, 56.7, 31.9, 31.9, 31.8, 31.6, 31.4, 31.4, 29.9, 29.5, 29.3, 29.3, 29.2, 28.0, 22.7, 14.1. ESI [(M+H)⁺]: *m/z* calculated for C₂₂H₃₉N₄⁺: 359.3; found: 359.3.

4.2. BIOLOGICAL EXPERIMENTS

4.2.1. Parasites. *L. amazonensis*-wild type (IFLA/BR/67/PH8) promastigotes were cultured in Warren's medium (brain–heart infusion plus hemin and folic acid), enriched with 10% fetal bovine serum (FBS, Cultilab). *L. amazonensis* (IFLA/BR/67/PH8) promastigotes transfected with the red fluorescent protein (RFP) were kept in 199 medium (Himedia AT014) supplemented with hemin, FBS, MEM vitamin solution (Thermo Fisher 11120052), and penicillin and streptomycin solution. The cells were maintained in BOD incubators at 25 °C.

4.2.2. Antileishmanial Activity against Promastigotes of *L. amazonensis*. The toxicity of imidazo-pyrimidine analogues in *L. amazonensis* promastigotes was assessed by the colorimetric 3-(4,5-dimethylthiazol-2-yl)-2,5-diphenyltetrazolic bromide (MTT) method (Sigma Chemical Co., St. Louis, MO, United States).³⁶ Briefly, promastigotes in the logarithmic growth phase were adjusted to a concentration of 2 × 10⁶ cells/mL in a culture medium. The parasites were exposed to different concentrations of the compounds (6.25–100 μM), for 72 h at 25 °C. Then, the MTT solution (5 mg/mL) was added, and after 4 h of incubation, the plates were read on a spectrophotometer at 570 nm. Untreated promastigotes were used as the negative control, and miltefosine was used as the reference drug. The percentage of viable parasites was determined by comparing treated cells with the untreated control. The IC₅₀ was calculated using the GraFit5 software (Erithacus Software Ltd., Horley, United Kingdom), using values obtained from three independent experiments.

4.2.3. Antileishmanial Activity against Amastigotes of *L. amazonensis*. Antileishmanial activity of compounds was evaluated in intracellular amastigotes of *L. amazonensis* RFP, by the fluorimetry method. To achieve this, macrophages were obtained from the peritoneal cavity of BALB/C mice after stimulus with thioglycolate medium (3%). Then, adherent macrophages were infected with stationary phase *L.*

*amazonensis*RFP promastigotes at a ratio of 10:1 (parasite per cell). After 4h, the wells were washed to eliminate non-phagocytosed parasites and treated with different concentrations of the compounds (12.5–100 μM). After 72 h of incubation at 33 °C with 5% CO₂, the cells were lysed with deionized water, and the contents of the wells were transferred to black 96-well transparent bottom plates. The plates were read on a fluorimeter at corresponding wavelengths of 540/600 nm of excitation and emission. Untreated macrophages were used as the negative control, and miltefosine was used as the reference drug. The values were expressed in an IC₅₀ of cell growth calculated using the average of three independent experiments. This protocol was approved by the Ethics Committee for Animal Research (CEUA) of Federal University of Juiz de Fora (no. 008/2018-CEUA).

4.2.4. Cytotoxicity in Murine Peritoneal Macrophages. The cytotoxicity of imidazo-pyrimidine analogues was determined by the MTT colorimetric method. Peritoneal macrophages were obtained as describe above. Then, adherent cells (2 × 10⁶ cells/mL) were treated with different concentrations (6.25–150 μM) of the compounds. After 72 h, the cells were incubated with MTT (5 mg/mL) for 2 h, and then, the plates were read on a spectrophotometer at 570 nm. Untreated macrophages were used as negative controls, and miltefosine was used as the reference drug. The results were expressed in a CC₅₀ of cell viability. This protocol was approved by the CEUA of Federal University of Juiz de Fora (no. 007/2018-CEUA).

4.3. IN SILICO PHYSICO-CHEMICAL, PHARMACOKINETIC, AND TARGET STUDIES

The SMILE notation of compound **24** was obtained using ChemSketch software (ACD/Laboratories 2020.1.2). The SMILE notation was inserted into the free online platform PKCSM available at the address <http://biosig.unimelb.edu.au/pkcsm/> to obtain data on physicochemical properties such as logP, molecular mass, HBD, and HBA sites. The results obtained were evaluated according to the Lipinski's rule of five (logP ≤ 5; M_w ≤ 500, HBA ≤ 5, and HBD ≤ 10). The ADMET profile was evaluated using the AdmetSAR software.³²

■ ASSOCIATED CONTENT

Supporting Information

The Supporting Information is available free of charge at <https://pubs.acs.org/doi/10.1021/acsomega.3c05441>.

Copies of ¹H NMR, ¹³C NMR, MS analysis for the synthesized compounds, HPLC purity analysis of the selected lead compounds and percent cell viability of compounds **18**, **22**, **24**, and **25** measured using an MTT assay (PDF)

■ AUTHOR INFORMATION

Corresponding Authors

Elaine S. Coimbra – Department of Parasitology, Microbiology and Immunology, Institute of Biological Sciences, Federal University of Juiz de Fora, Juiz de Fora 36036-900, Brazil; Email: elaine.coimbra@ufjf.edu.br

Deepak B. Salunke – Department of Chemistry and Centre of Advanced Studies in Chemistry, Panjab University, Chandigarh 160 014, India; National Interdisciplinary Centre of Vaccine, Immunotherapeutic and Antimicrobials,

Panjab University, Chandigarh 160 014, India;
orcid.org/0000-0002-1241-9146; Email: salunke@pu.ac.in

Authors

Ravinder Kumar – Department of Chemistry and Centre of Advanced Studies in Chemistry, Panjab University, Chandigarh 160 014, India

Rahul Singh – Department of Chemistry and Centre of Advanced Studies in Chemistry, Panjab University, Chandigarh 160 014, India

Ayla das Chagas Almeida – Department of Parasitology, Microbiology and Immunology, Institute of Biological Sciences, Federal University of Juiz de Fora, Juiz de Fora 36036-900, Brazil

Juliana da Trindade Granato – Department of Parasitology, Microbiology and Immunology, Institute of Biological Sciences, Federal University of Juiz de Fora, Juiz de Fora 36036-900, Brazil

Ari Sérgio de Oliveira Lemos – Department of Parasitology, Microbiology and Immunology, Institute of Biological Sciences, Federal University of Juiz de Fora, Juiz de Fora 36036-900, Brazil

Kushvinder Kumar – Department of Chemistry and Centre of Advanced Studies in Chemistry, Panjab University, Chandigarh 160 014, India

Madhuri T. Patil – Mehr Chand Mahajan DAV College for Women, Chandigarh 160036, India

Adilson D. da Silva – Department of Chemistry, Institute of Exact Sciences, Federal University of Juiz de Fora, 36036-900 Juiz de Fora, Brazil

Ambadas B. Rode – Regional Centre for Biotechnology, NCR Biotech Science Cluster, Faridabad 121 001, India;
orcid.org/0000-0002-7252-0385

Complete contact information is available at:
<https://pubs.acs.org/10.1021/acsomega.3c05441>

Notes

The authors declare no competing financial interest.

ACKNOWLEDGMENTS

Deepak B. Salunke is thankful to DBT New Delhi for the award of the Ramalingaswami Fellowship (BT/RLF/Re-entry/16/2013) and Science and Engineering Research Board (SERB), New Delhi for the Core Research Grant (CRG/2021/005467), Department of Science & Technology & Renewable Energy, Chandigarh Administration, Paryavaran Bhawan, Chandigarh for Short Term Research Project, and Indian Council of Medical Research, New Delhi for the ad hoc research project. M.T.P. is thankful to DST for the award of Women Scientist Scheme-A [SR/WOS-A/CS-132/2016 (G)]. SAIF/CIL of Panjab University is gratefully acknowledged. We are grateful to the Brazilian funding agencies, Conselho Nacional de Desenvolvimento Científico e Tecnológico (CNPq, Brazil), Fundação de Amparo a Pesquisa de Minas Gerais (FAPEMIG, Brazil), Coordenação de Aperfeiçoamento de Pessoal de Nível Superior (CAPES, Brazil), and Universidade Federal de Juiz de Fora (UFJF, Brazil). E.S.C. and A.D.S. are research productivity fellows from CNPq. The authors are grateful to the Center for Reproduction Biology (CBR/UFJF) for the animals.

REFERENCES

- (1) WHO 2023. *Epidemiological situation*. <http://www.who.int/leishmaniasis/burden/en/> (accessed May 2023).
- (2) Ruiz-Postigo, J. A.; Grouta, L.; Saurabh, J. 2020. *Global leishmaniasis surveillance, 2017–2018, and first report on 5 additional indicators*. <https://www.who.int/publications-detail-redirect/who-wer9525> (accessed May 2023).
- (3) Carvalho, S. H.; Frézard, F.; Pereira, N. P.; Moura, A. S.; Ramos, L. M. Q. C.; Carvalho, G. B.; Rocha, M. O. C. American tegumentary leishmaniasis in Brazil: a critical review of the current therapeutic approach with systemic meglumine antimoniate and short-term possibilities for an alternative treatment. *Trop. Med. Int. Health* **2019**, *24*, 380–391.
- (4) Chakravarty, J.; Sundar, S. Current and emerging medications for the treatment of leishmaniasis. *Expert Opin. Pharmacother.* **2019**, *20*, 1251–1265.
- (5) Elmahallawy, E. K.; Agil, A. Treatment of leishmaniasis: a review and assessment of recent research. *Curr. Pharmaceutical Design* **2015**, *21*, 2259–2275.
- (6) Castera-Ducros, C.; Paloque, L.; Verhaeghe, P.; Casanova, M.; Cantelli, C.; Hutter, S.; Tanguy, F.; Laget, M.; Remusat, V.; Cohen, A.; Crozet, M. D.; Rathelot, P.; Azas, N.; Vanelle, P. Targeting the human parasite *Leishmania donovani*: Discovery of a new promising anti-infectious pharmacophore in 3-nitroimidazo[1,2-a]pyridine series. *Bioorg. Med. Chem.* **2013**, *21*, 7155–7164.
- (7) Marhadour, S.; Marchand, P.; Pagniez, F.; Bazin, M.-A.; Picot, C.; Lozach, O.; Ruchaud, S.; Antoine, M.; Meijer, L.; Rachidi, N.; Le Pape, P. Synthesis and biological evaluation of 2,3-diarylimidazo[1,2-a]pyridines as antileishmanial agents. *Eur. J. Med. Chem.* **2012**, *58*, 543–556.
- (8) Allocco, J. J.; Donald, R.; Zhong, T.; Lee, A.; Tang, Y. S.; Hendrickson, R. C.; Liberator, P.; Nare, B. Inhibitors of casein kinase 1 block the growth of *Leishmania major* promastigotes in vitro. *Int. J. Parasitology* **2006**, *36*, 1249–1259.
- (9) Hernández, P.; Rojas, R.; Gilman, R. H.; Sauvain, M.; Lima, L. M.; Barreiro, E. J.; González, M.; Cerecetto, H. Hybrid furoxanyl N-acylhydrazone derivatives as hits for the development of neglected diseases drug candidates. *Eur. J. Med. Chem.* **2013**, *59*, 64–74.
- (10) Dichiarà, M.; Simpson, Q. J.; Quotadamo, A.; Jalani, H. B.; Huang, A. X.; Millard, C. C.; Klug, D. M.; Tse, E. G.; Todd, M. H.; Silva, D. G.; da Silva Emery, F.; Carlson, J. E.; Zheng, S.-L.; Vleminckx, M.; Matheeußen, A.; Caljon, G.; Pollastri, M. P.; Sjö, P.; Perry, B.; Ferrins, L. *ACS Infectious Diseases* **2023**, *9*, 1470–1487.
- (11) Weber, L. The application of multi-component reaction in drug discovery. *Curr. Med. Chem.* **2002**, *9*, 2085–2093.
- (12) Devi, N.; Rawal, R. K.; Singh, V. Diversity-oriented synthesis of fused-imidazol derivatives via Groebke-Blackburn-Bienaymé reaction. *Tetrahedron* **2015**, *71*, 183–232.
- (13) Shaaban, S.; Abdel-Wahab, B. F. Groebke–Blackburn–Bienaymé multicomponent reaction: emerging chemistry for drug discovery. *Mol. Diversity* **2016**, *20*, 233–254.
- (14) Liu, Z. Q. Discovery of novel imidazo [1,2-a]-involved N-Heterocyclic drugs by Groebke-Blackburn-Bienaymé three-component-reaction. *Mini-Rev. Org. Chem.* **2016**, *13*, 166–183.
- (15) Singh, R.; Pandrala, M.; Malhotra, S. V.; Pawar, G. P.; Chaudhari, V. D.; Salunke, D. B. Design, synthesis, anti-cancer screening and structure activity of biphenyl relationship studies linked fused imidazoles. *J. Ind. Chem. Soc.* **2020**, *97*, 1237–1244.
- (16) Shukla, N. M.; Salunke, D. B.; Yoo, E.; Mutz, C. A.; Balakrishna, R.; David, A. S. Antibacterial activities of Groebke–Blackburn–Bienaymé-derived imidazo[1,2-a]pyridin-3-amines. *Bioorg. Med. Chem.* **2012**, *20*, 5850–5863.
- (17) Kaur, M.; Singh, R.; Patil, M. T.; Kumar, K.; Sahoo, S. C.; Singh, K. N.; Chaudhari, V. D.; Salunke, D. B. Microwave-assisted Groebke-Blackburn-Bienaymé multicomponent reaction to synthesize imidazo fused heterocycles via in-situ generated isocyanides from N-formylamines: An undergraduate organic laboratory experiment. *J. Het. Chem.* **2021**, 1–10.

- (18) Boltjes, A.; Domling, A. Groebke-Blackburn-Bienaymé reaction. *Eur. J. Org. Chem.* **2019**, *2019*, 7007–7049.
- (19) Singh, R.; Kumar, R.; Kaur, M.; Patil, M. T.; Sahoo, S. C.; Salunke, D. B. Groebke-Blackburn-Bienaymé Multicomponent Reaction Coupled with Unconventional Pictet-Spengler Cyclization for the Synthesis of Imidazo[4,5-*b*]pyridine Fused Polycyclic Heterocycles. *J. Het. Chem.* **2022**, 1–9.
- (20) Salunke, D. B.; Yoo, E.; Shukla, N. M.; Balakrishna, R.; Malladi, S. S.; Serafin, K. J.; Day, V. W.; Wang, X.; David, S. A. Structure–Activity Relationships in Human Toll-like Receptor 8-Active 2,3-Diamino-furo[2,3-*c*]pyridines. *J. Med. Chem.* **2012**, *55*, 8137–8151.
- (21) Kuettel, S.; Zambon, A.; Kaiser, M.; Brun, R.; Scapozza, L.; Perozzo, R. Synthesis and Evaluation of Antiparasitic Activities of New 4-[5-(4-Phenoxyphenyl)-2H-pyrazol-3-yl]morpholine Derivatives. *J. Med. Chem.* **2007**, *50*, 5833–5839.
- (22) Ahsan, M.; Ansari, M.; Kumar, P.; Soni, M.; Yasmin, S.; Jadav, S.; Sahoo, G. C. In vitro studies of the antileishmanial activity of the newer 2-(substitutedphenoxy)-N-[(aryl)methylidene]acetohydrazide analogues. *Beni-Suef University Journal of Basic and Applied Sciences* **2016**, *5*, 119–125.
- (23) Khan, K. M.; Khan, M. Z.; Taha, M.; Maharvi, G. M.; Saify, Z. S.; Parveen, S.; Choudhary, M. I. Leishmanicidal potential of N-substituted morpholine derivatives: Synthesis and structure–activity relationships. *Nat. Prod. Res.* **2009**, *23*, 479–484.
- (24) Wylie, S.; Brand, S.; Thomas, M.; De Rycker, M.; Chung, C.; Pena, I.; Bingham, R. P.; Bueren-Calabuig, J. A.; Cantizani, J.; Cebrian, D.; Craggs, P. D.; Ferguson, L.; Goswami, P.; Hobrath, J.; Howe, J.; Jeacock, L.; Ko, E.-J.; Korczynska, J.; MacLean, L.; Manthri, S.; Martinez, M. S.; Mata-Cantero, L.; Moniz, S.; Nühs, A.; Osuna-Cabello, M.; Pinto, E.; Riley, J.; Robinson, S.; Rowland, P.; Simeons, F. R. C.; Shishikura, Y.; Spinks, D.; Stojanovski, L.; Thomas, J.; Thompson, S.; Viayna Gaza, E.; Wall, R. J.; Zuccotto, F.; Horn, D.; Ferguson, M. A. J.; Fairlamb, A. H.; Fiandor, J. M.; Martin, J.; Gray, D. W.; Miles, T. J.; Gilbert, I. H.; Read, K. D.; Marco, M.; Wyatt, P. G. Preclinical candidate for the treatment of visceral leishmaniasis that acts through proteasome inhibition. *Proc. Natl. Acad. Sci. USA* **2019**, *116*, 9318–9323.
- (25) Escobar, P.; Matu, S.; Marques, C.; Croft, S. L. Sensitivities of *Leishmania* species to hexadecylphosphocholine (miltefosine), ET-18-OCH(3) (edelfosine) and amphotericin B. *Acta Tropica* **2002**, *81*, 151–157.
- (26) Vermeersch, M.; da Luz, R. I.; Toté, K.; Timmermans, J. P.; Cos, P.; Maes, L. In vitro susceptibilities of *Leishmania donovani* promastigote and amastigote stages to antileishmanial reference drugs: practical relevance of stage-specific differences. *Antimicrob. Agents Chemother.* **2009**, *53*, 3855–3859.
- (27) De Muylder, G.; Ang, K. K.; Chen, S.; Arkin, M. R.; Engel, J. C.; McKerrow, J. H. A screen against *Leishmania* intracellular amastigotes: comparison to a promastigote screen and identification of a host cell-specific hit. *PLoS Neglected Trop. Dis.* **2011**, *5*, No. e1253.
- (28) Baek, K. H.; Piel, L.; Rosazza, T.; Prina, E.; Späth, G. F.; No, J. H. Infectivity and Drug Susceptibility Profiling of Different *Leishmania*-Host Cell Combinations. *Pathogens* **2020**, *9*, 393.
- (29) Singh, R.; Kumar, R.; Pandrala, M.; Kaur, P.; Gupta, S.; Tailor, D.; Malhotra, S. V.; Salunke, D. B. Facile synthesis of C6-substituted benz[4,5]imidazo[1,2-*a*]quinoxaline derivatives and their anticancer evaluation. *Archiv der Pharmazie* **2021**, *354*, 2000393.
- (30) Lipinski, C. A.; Lombardo, F.; Dominy, B. W.; Feeney, P. J. Experimental and computational approaches to estimate solubility and permeability in drug discovery and development settings. *Adv. Drug Delivery Rev.* **2001**, *46*, 3–26.
- (31) Lipinski, C. A. Lead- and drug-like compounds: the rule-of-five revolution. *Drug Discovery Today: Technologies* **2004**, *1*, 337–341.
- (32) Pires, D. E. V.; Blundell, T. L.; Ascher, D. B. pkCSM: Predicting Small-Molecule Pharmacokinetic and Toxicity Properties Using Graph-Based Signatures. *J. Med. Chem.* **2015**, *58*, 4066–4072.
- (33) Ruela, A. L. M.; Perissinato, A. G.; Lino, M. E. S.; Mudrik, P. S.; Pereira, G. R. Evaluation of skin absorption of drugs from topical and transdermal formulations. *Brazilian J. Pharm. Sci.* **2016**, *52*, 527–544.
- (34) Almazroo, O. A.; Miah, M. K.; Venkataramanan, R. *Drug Metabolism in the Liver Clin Liver Dis* **2017**, *21*, 1–20.
- (35) Motohashi, H.; Inui, K. I. Organic Cation Transporter OCTs (SLC22) and MATes (SLC47) in the Human Kidney. *AAPS Journal* **2013**, *15*, 581–588.
- (36) Mosmann, T. Rapid colorimetric assay for cellular growth and survival: Application to proliferation and cytotoxicity assays. *J. Immunol. Methods* **1983**, *65*, 55–63.